Quantum Stud.: Math. Found. (2018) 5:5–21
https://doi.org/10.1007/s40509-017-0128-8

CHAPMAN UNIVERSITY | INSTITUTE FOR QUANTUM STUDIES

REGULAR PAPER

Conventional/unconventional superconductivity in high-pressure hydrides and beyond: insights from theory and perspectives

Luciano Pietronero · Lilia Boeri · Emmanuele Cappelluti · Luciano Ortenzi

Received: 18 August 2017 / Accepted: 23 August 2017 / Published online: 9 September 2017

Abstract The observation of a superconducting critical temperature T_c exceeding 200K in ultra-dense hydrogen sulfide has demonstrated that high-T_c superconductivity can be achieved also in compounds where the superconducting pairing is mediated by phonons. This poses interesting challenges and opportunities. In particular, in this paper, we present a theoretical overview of the following points:

– Density functional theory has been quite effective in predicting various structures and this was the first time that theory has been successful in predicting novel superconductors. Along this line, we use DFT and many body theory to discuss possible strategies to search for new high-T_c superconductors in light-element compounds at high pressures [20,34,36,37,43].
– The microscopic key elements for high T_c seem to be a high phonon frequency, a peak in the density of states, a large el-ph coupling due to strong bonds, and the avoidance of lattice instabilities for very large couplings. The first two points lead to an appreciable Migdal parameter and to the possibility that non-adiabatic effects may require the generalization of the standard Migdal–Eliashberg theory of superconductivity [32,33,45].
– In this perspective, it would be important to locate these materials in the Uemura diagram and to measure isotope effect for T_c but also for the effective electron mass and the magnetic susceptibility [31], where the standard ME theory would give zero effect.
– The possibility of going beyond ME theory adds a new dimension also in the perspective of exporting these concepts to other materials at ambient or low pressure. For example, carbon compounds have a phonon frequency similar to the hydrides and the coupling can also be strong. This points to a search towards fullerene, graphene, or doped graphane. In these materials, especially fullerene, the Fermi energy is very small and the system is certainly in the non-adiabatic regime [31–33,45].

Keywords H_3S · High T_c superconductivity · Hydrides

L. Pietronero (✉)· L. Boeri
Dipartimento di fisica, "Sapienza" Universita' di Roma, p.le Aldo Moro 5, 00185 Rome, Italy
e-mail: luciano.pietronero@roma1.infn.it; luciano.ortenzi@sapienza.isc.cnr.it

L. Pietronero · E. Cappelluti · L. Ortenzi
Istituto dei sistemi complessi (ISC)-CNR, via dei Taurini 19, 00185 Rome, Italy

1 Introduction

The discovery of high-T_c superconductivity in H_3S at the end of 2014 has changed the perception of superconductivity research under many points of view [17]. First, it proved that high-T_c superconductivity can be achieved within a phonon-mediated scenario, and does not require an exotic mechanism, as conjectured in cuprates and pnictides. Second, it demonstrated that ranges of chemical compositions, pressure, etc. conducive to high T_c can be predicted from the first principles, offering a very powerful tool for materials research [19]. It is not surprising, then, that this discovery has stimulated a lot of activity, both on the theoretical and experimental sides. The first *Superhydrides* meeting, which was held in Rome in 2016, was a timely opportunity to discuss the recent advancements in the field, with many exciting contributions. One year later, the situation is still evolving: the initial challenge of understanding superconductivity in H_3S has turned into general principles, which could lead to the discovery of other superconductors. The main challenges that theory faces at this point are essentially of two types:

1. What makes superconductivity in H_3S special or, better, is H_3S really a "standard" conventional superconductor?
2. Is it possible to design other superconductors with improved superconducting characteristics, i.e., higher T_cs or lower pressures?

In this contribution, we present our view on these two issues. We start with a short overview of the arguments leading to the H_3S discovery (Sect. 2), and then discuss the main technical aspects of ab initio material prediction, with an overview of the current situation in the field (Sect. 3); we consider, in some detail, the origin and properties of the Van Hove singularities in the band structure of H_3S (Sect. 4) and we then discuss the main aspects which make H_3S stand out from other conventional superconductors, and which may require an extension of standard Migdal–Eliashberg (ME) approaches (Sect. 5) , with a special emphasis of non-adiabatic (beyond Born–Oppenheimer) effects. In Sect. 6, we discuss the Uemura diagram suggesting to locate H_3S on this diagram. Finally, in Sect. 7, we suggest some paths for material optimization at low pressure.

2 Why H_3S is special

The discovery of superconductivity in H_3S has a long history, going back to the late sixties, when Neil Ashcroft predicted that metallic hydrogen could become a room-temperature superconductor [5]. At that time, the prediction was impossible to verify, since the pressures required to metallized hydrogen were too high for the experimental knowledge at the time. Ashcrofts simple argument descended directly from the conventional theory of superconductivity (Migdal–Eliashberg theory), which predicts that the critical temperature (T_c) of a superconductor can be approximated by the formula:

$$T_c = \frac{\omega_{ln}}{1.2} \exp\left(\frac{-1.04}{\lambda - \mu^*(1 + 0.62\lambda)}\right), \tag{1}$$

where ω_{ln} and λ measure, respectively, the weighted average of the phonon spectrum of a material , and the intensity of the electron–phonon (ep) coupling, and μ^* is the so-called Coulomb pseudopotential. These quantities are moments of the electron–phonon (Eliashberg) spectral function, and involve function of the electronic and phononic spectrum, and of the electron–phonon matrix elements [12]. Essentially, metallic hydrogen should exhibit a high T_c, because its small mass would ensure large phonon frequencies, and hence a large prefactor in the T_c formula (1). A metallic state is essential, because the electron–phonon coupling constant λ is proportional to the Density of States at the Fermi level, through the so-called Hopfields formula:

$$\lambda = \frac{N(E_F)I^2}{M\omega^2}, \tag{2}$$

where $N(E_F)$ is the density of states at the Fermi level (E_F), I is the average ep matrix element, and ω is an average phonon frequency. Although Ashcrofts arguments were quite simple and sensible, they were ignored for a long time. One reason is probably that, as we mentioned, the metallization of hydrogen was deemed almost impossible at the time. The second reason is most likely the so-called Cohen–Anderson (CA) limit, which caused a prejudice on the conventional superconductors that remains until today [13]. The CA limit is based on the fact that, besides pairing electrons, ep interaction also leads to a softening of the phonon spectrum, which can ultimately lead to lattice instabilities. Based on typical parameters of the best materials known in the 70s, this resulted in a maximum T_c of around 25 K, which in fact remained unsurpassed for more than 40 years. Even the discovery of the high-T_c cuprates in 1986 was not in contradiction with this idea, because, although these materials, they are clearly not described by the conventional ME theory [7]. T_cs are as high as 156 K. Other compounds in this class are Fe pnictides and chalcogenides, where T_cs as high as 100 K have been reported in monolayers [35].

An important turning point in this search of new conventional superconductors was the discovery of a T_c of 39 K in MgB_2: [42] this material, which is a simple metal formed by two s-p elements, magnesium and boron. MgB_2 was clearly not an exotic compound, like cuprates and pnictides, but, nevertheless, its T_c was higher than the CA limit. Indeed, many of the characteristics of MgB_2 are strongly anomalous compared to the Matthias' rules that guided the search for new conventional superconductors: instead of being a transition metal compound with high peaks in the DOS, like the A_{15}-large N(E_F) in Eq. (2)—MgB_2 is a covalent metal, in which the electron–phonon coupling is large because of intrinsically large ep matrix elements (I) [4].

Covalent metals are extremely rare at ambient pressures, but after MgB_2, a few other examples were experimentally observed (boron-doped diamond and silicon) [11,21] or predicted, such as LiBC, LiB, and graphane [38,47,48]

The concept of covalent metals and light-element compounds led Ashcroft to revisit his original idea and formulate a second, even more insightful, prediction. Instead of exploring the high-pressure behavior of pure hydrogen, in 2004, he proposed looking at the high-pressure phase diagram of covalent hydrogen-rich compounds (hydrides). The idea is that impurities in the hydrogen matrix would exert a chemical pressure on the hydrogen lattice, thus reducing the pressure needed for metallization. 35 years later, the progress of the experimental techniques was such that the prediction could actually be tested. In 2008, the group of Mikhail Eremets measured superconductivity in compressed silane (SiH4), but the T_c was disappointingly low [22].

High-pressure resistivity measurements are extremely delicate, and the somehow disappointing result on silane showed that not all hydrides are high-T_c superconductors. What was needed was a reasonably accurate guess of the ranges of pressure and chemical compositions for high-T_c superconductivity. Fortunately, the recent progress in ab initio methods for crystal structure prediction and superconductivity went precisely in this direction [40,53], allowing for an accurate, parameter-free calculation of the high-pressure phase diagrams of elements and compounds. In 2009, a very influential paper by Zurek et al. pointed out another distinctive characteristic of the high-pressure phase diagrams of hydrides at high pressure, namely, the formation of so-called superhydrides, i.e., binary phases that have an increased hydrogen content compared to the nominal valence [55]. These phases, which can be considered a special example of high-pressure forbidden chemistry, exhibit a variety of bonding environments and physical behaviors, including covalent metallic behavior. It was then obvious to try and exploit superhydrides for high-T_c superconductivity.

A few spectacular predictions were made; Ca hydride was predicted to exhibit a T_c exceeding 200 K.[52]. Although this specific prediction was never verified, a second, extremely accurate prediction followed for sulfur hydride: Duan et al. showed that under sufficient compression in hydrogen atmosphere, sulfur hydride, (SH2), which forms a molecular crystal under pressure, should first incorporate hydrogen into the lattice transforming into SH_3, and then undergo several structural transitions towards more symmetric structures. Around 100 GPa SH_3 would become metallic and superconducting with a maximum T_c of 203 K at 200 Gpa. The maximum T_c is achieved in the $Im3-m$ structure shown in Fig. 1; the isocontours of the Electronic Localization Function (ELF) superimposed to the structure show that highly covalent, similar to what observed in MgB_2 and other superconductors. After SH_3, high-T_c has been reported also in another binary hydride (PH3), and it is likely that others will be reported soon.

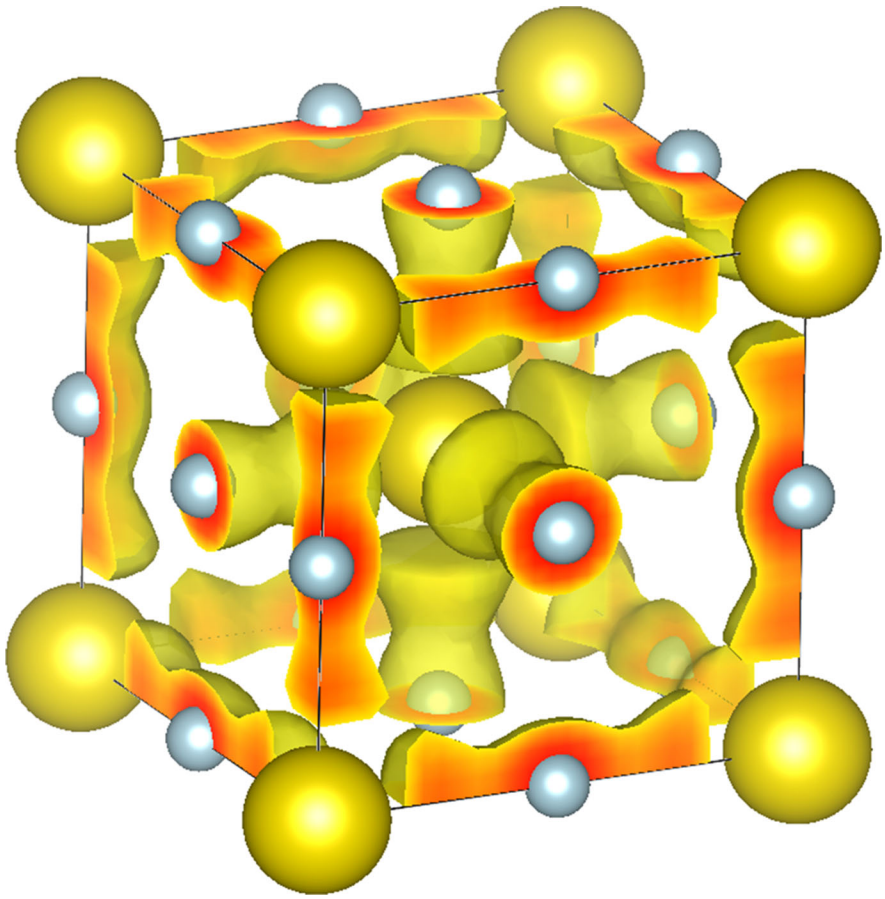

Fig. 1 Crystal structure of the high-pressure high-T_c phase of H_3S; sulfur atoms are shown in *yellow* and hydrogen in *white*. An isocontour of the electronic localization function is superimposed to the figure

The picture from theoretical predictions is quite clear: only a small fraction of binary hydrides should exhibit high-T_c superconductivity, and SH_3 is almost optimal, since in this case, three parameters are maximum. However, many more possibilities exist considering multinary hydrides, metastable phases, and other light-element compounds. In addition to "chemical" effects, other routes to high T_c include the optimization of non-adiabatic pairing channels. We will illustrate these strategies in the next sections.

3 Phase diagram and material prediction

Methods for ab initio crystal structure prediction played a fundamental role in the SH_3 discovery, and most likely will increasingly drive the search for new superconductors in the future. The field has seen a very rapid expansion in the last 10 years, and in many cases, modern methods reach an accuracy which is comparable to that of experiments. Their role is particularly important in all cases in which experiments are hard to perform, as in the case of diamond anvil cell experiments in the Megabar range. Before describing the main applications to the search for new superconductors, we describe the basic working principle. Predicting the crystal structure of a material for a given regime of chemical composition and pressure amounts to finding the global minimum of a complicated landscape, generated by the ab initio total energies (or enthalpies) of all possible crystal structures. The number of possible configurations for a typical problem is so large that a purely enumerative approach is unfeasible: for example, the total number of different configurations for a binary alloy in which the two atoms are allowed to occupy any position on a

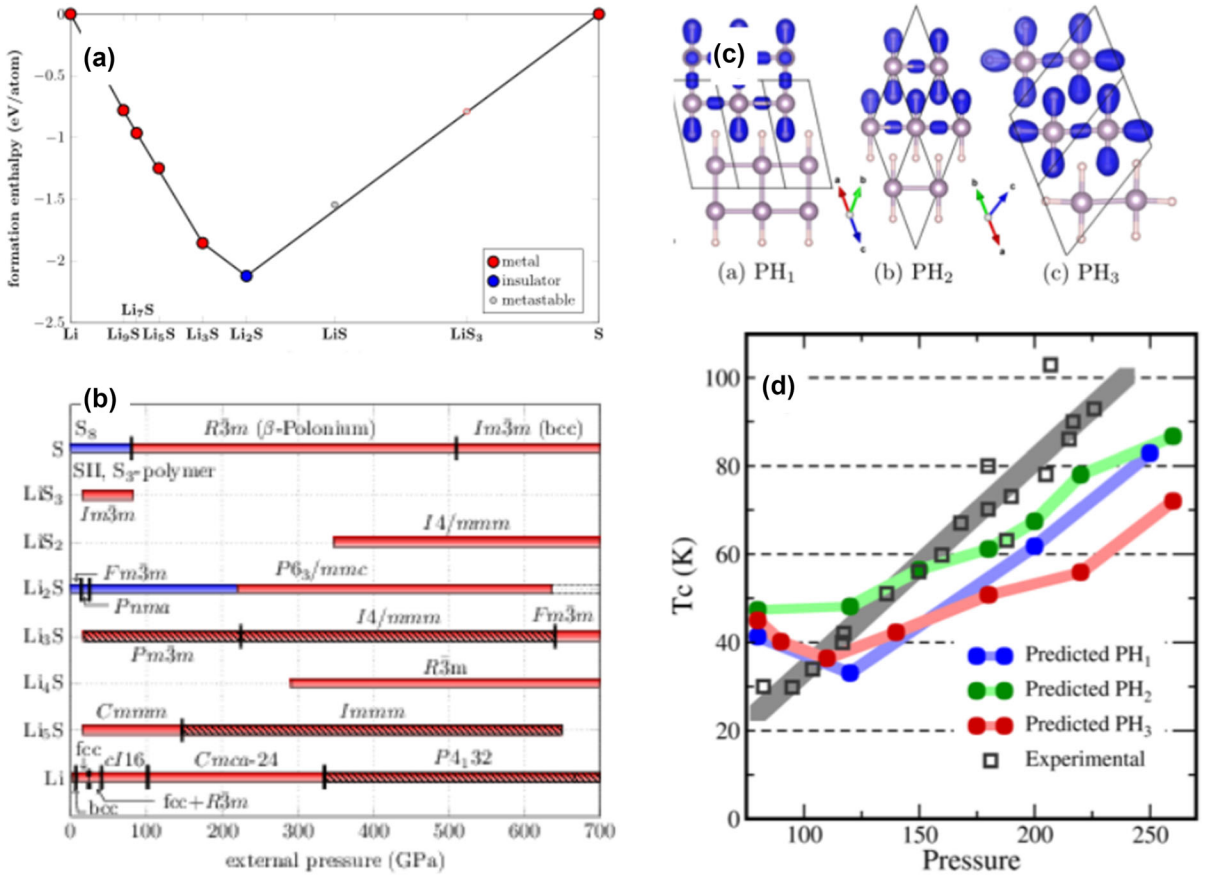

Fig. 2 Convex hulls of stability (**a**) and high-pressure phase (**b**) of the Li–S system; **c** High-pressure crystal structures of phosphines (PH_x) predicted with ab initio crystal structure search; **d** calculated and experimental T_c for phosphines under pressures from refs. [25,37]

discrete grid with a spacing of 0.5 Åin a cubic unit cell with an edge of 10 Åis 1012! However, several methods have been developed to efficiently sample the energy hypersurface, immensely reducing the computational time, such as ab initio random structure search, minima hopping, metadynamics, genetic algorithms, etc, [53]. Once the most favorable crystal structure for a given composition and pressure is known, the ab initio Calphad (CALculation of PHAse Diagrams) approach permits to predict accurate phase diagrams and even chemical reactions, such as catalysis, hydrogen intake in metals and alloys, etc. [41].

The combination of ab initio crystal structure prediction and thermodynamics with ab initio superconductivity calculations has permitted to identify many new superconducting hydrides. The basic working principle is illustrated in Fig. 2, using figures extracted from our refs. [25,37]. Panel (a) is a typical convex hull construction, which is used to estimate the thermodynamic stability of different phases as a function of pressure. The points represent the formation enthalpy (H) of the lowest energy structure predicted by an evolutionary search for a given composition; for a binary phase with composition A_xB_y, H is defined as follows: $H = H(A_xB_y) - xH(A) - yH(B)$. If this quantity is negative, the phase A_xB_y is stable with respect to elemental decomposition; if it is positive, the phase is highly (or weakly) metastable, i.e., if formed, it will decompose into its elemental constituents in finite time. However, the decomposition into the two elements is often not the relevant one, as a compound could decompose into other phases, preserving the correct stoichiometry. To estimate all possible decompositions for the binary system, one constructs the most convex connecting the formation enthalpy of all known phases for a given stoichiometry. Points

on this convex hull represent stable compositions into which phases above the convex hull will decompose into given a sufficient interval of time.

The convex hull construction can be easily extended to multinary systems and to finite temperatures. Repeating the convex hull construction at different pressures, one can construct a phase diagram showing the stability ranges of different phases—panel (b). The most interesting crystal structures can then be further investigated, computing the trends of the critical temperature as a function of pressure. In some cases, the agreement between theory and experiment is remarkable (panels c–d). Panel (d) of Fig. 2 shows a comparison between experimental and theoretical superconducting trends in compressed phosphines, taken from Ref. [25]. Experimental T_cs are from resistivity measurements in Ref. [16], while calculations are performed within superconducting density functional theory (SCDFT), with a full inclusion of Coulomb screening effects, using structures predicted with the minima hopping method.

Given the large number of theoretical predictions on high-pressure superconducting hydrides in the last few years, it is impossible to give a full account. In the following, we will focus on our own results, and refer the reader to one of the most updated reviews [18,50] for details on other calculations. One of the most remarkable findings is that, despite the large number of compounds, genuinely high-T_c superconductivity in high-pressure hydrides is extremely rare; only a few predictions [39,52] surpass the T_c of SH_3, and only another hydride, phosphorus hydride (PH_3), was shown to superconduct at high T_c. The extreme scarcity of genuinely high-T_c phases is related to the difficulty of creating metallic covalent bonds, which are extremely rare also at high pressures. A key factor for the formation of metallic covalent bonds is an optimal electronegativity of the non-hydrogen atom: very electronegative elements tend to form hydrides that remain insulating up to very high pressures, while weakly electronegative elements form weak hydrides with low T_c's. The optimal choice are elements like sulfur, which have electronegativities close or slightly larger than hydrogen [8,28,34].

In Ref. [34], we tested this hypothesis using linear response calculations in the virtual crystal approximation for a series of compounds with chemical formula XH_3, where X is either a chalcogen (O, S, Se, and Te) or a virtual atom constructed from a linear combination of the two chalcogens. We revealed that, indeed, SH_3 is close to a "sweet spot" for superconductivity, but T_c could be increased by a moderate (<30%) doping with oxygen, making the H-X bond more ionic. Moving away from the chalcogens, one of the most obvious choices are pnictogens (elements of the V group). In particular, phosphorus has one electron less than sulfur and is its immediate neighbor in the periodic table, and forms a very reactive hydride (phosphine), with chemical formula PH_3. Under pressure, phosphine becomes metallic at around and superconducting around 40 GPa. The maximum T_c (100 K), is reached at around 200 GPa—see Fig. 2c. The experimental superconducting trends are with several new high-pressure PH_x phases, with $x = 1, 2, 3$, predicted by the minima hopping method. However, at variance with sulfur hydride, where SH_3 represents a clear minimum of the convex hull at high pressures, none of the new PH_x phases is thermodynamically stable with respect to elemental decomposition, according to DFT calculations [25,28,49]. Although this result is confusing at first sight, it is actually consistent with recent reports of rapid degradation of the samples in experiment [16].

The same mass argument behind high-T_c conventional superconductivity in hydrides applies to any compounds containing light elements, such as lithium, boron, carbon, etc. Lithium ($Z = 3$) is the next lightest element after hydrogen and helium; sitting just below hydrogen in the periodic table is an almost obvious choice for high-T_c superconductivity. In Ref. [37], we studied the high-pressure phase diagram of the Li-S system, using evolutionary methods for ab initio crystal structure prediction and linear response calculations of the electron–phonon coupling. We found that, similar to the H–S phase diagram, also in this system, several chemically-forbidden phases, besides the ambient-pressure Li_2S, are stabilized at high pressures. Their physical behavior is profoundly different from the corresponding hydrides, because of avoided core overlap effects, which are detrimental to superconductivity. Only at very high pressures ($P > 500$ GPa) do we find phases with strong Li–S bonds, and superconducting properties comparable to hydrides. Avoided core overlap effects most likely limit the superconducting critical temperatures of other known compounds of alkali metals at high pressures [54].

The possibilities of increasing the T_c in binaries are limited, but ternary (and multinary) systems offer a much larger flexibility. On the other hand, the calculation of ternary (or higher) phase diagrams is much more involved, because

it requires taking into account all possible decomposition paths; therefore, ab initio studies of ternary hydrides are at the moment rare. Flores-Livas et al. [27] proposed to dope ice with group-*III* and group-*V* elements to achieve high T_c. Nitrogen is the best dopant leading to T_cs up to 60 K. Flores-Livas et al.'s calculations treat doping using supercells of the ice *X*, but do not perform a full search of the ternary phase diagram, which would be prohibitive for small dopant concentrations.

In Ref. [37], we performed one of the first studies of the full ternary phase diagram of a complex hydride, considering the ternary Li–B–H system. This system is of particular interest, because the ground-state structure at ambient conditions, $LiBH_4$, is one of the best materials for hydrogen-storage applications. This phase remains a wide band-gap insulator at all pressures investigated. Other phases along the 1:1:*x* Li:B:H line are also insulating. However, a full search of the ternary phase diagram at 200 GPa revealed a metallic Li_2BH_6 phase, which is thermodynamically stable down to 100 GPa. This superhydride phase, crystallizing in a Fm_3m space group, is characterized by sixfold hydrogen-coordinated boron atoms occupying the fcc sites of the unit cell. Due to strong hydrogen- boron bonding, this phase displays a critical temperature of 100 K between 100 and 200 GPa. These findings indicate that ternary compounds used in hydrogen-storage applications are a suitable choice for observing high-T_c conventional superconductivity in diamond anvil cell experiments, and suggest a viable route to optimize the critical temperature of high-pressure hydrides.

Metastable phases, which explain the superconductivity in PH_3, most likely play an important role in the high-pressure superconducting phase diagram of many compounds. In Ref. [26], we studied the high-pressure phase diagram of phosphorus, which is one of the most complex among the elements. Using resistivity measurements combined with ab initio superconductivity calculations, we solved for the first time the open controversies on the anomalous superconducting trends, within a single, consistent scenario of multiple metastable structures which coexist beyond their thermodynamical stability range.

The main results are shown in Fig. 3. The upper panel reports the superconducting T_c from resistivity measurements in diamond anvil cells, obtained using two different procedures: In the first set (Exp 1, full curve), the sample is constantly kept at low temperature, while pressure is increased. In the second P-T path (Exp. 2, dashed curve), the temperature is raised at higher temperatures when applying pressure for resistivity measurements. The dependence of T_c on the pressure cycle indicates a likely coexistence of two different metastable phases at low pressures, which collapse onto a single curve for $P > 25$ GPa. This is confirmed by ab initio calculations, as shown in the lower panel of the figure. Here, SCDFT T_cs for different allotropes which are predicted to be stable (full lines) or metastable (dashed lines) in different pressure ranges are shown in different colors.

At low pressure, the coexistence of black phosphorus (black) with a rhombohedral ($R3m$) phase, which collapse onto the simple cubic (sc) phase at 25 GPa, reproduce the bifurcation of T_c seen in experiment. We predict that a similar behavior could be observed at higher pressures, where stable and metastable structures exhibit clearly distinct superconducting trends. Note that metastable structures systematically exhibit critical temperatures which are distinctively higher than the putative ground-state structures. This suggests that the selective stabilization of metastable phases represents a viable strategy to improve superconductivity properties of the conventional superconductors. A similar mechanism may be behind the recent controversial reports of metallization in hydrogen [14,15,23].

3.1 Are things really so normal?

The arguments discussed so far on H_3S and other high-pressure hydrides are based on the assumption that superconductivity in these compounds is completely conventional, i.e., that the standard Migdal–Eliashberg theory for superconductors can be safely applied [3]. This is mainly based on the excellent agreement between the first theoretical prediction for T_c and the measurements in H_3S [17,19]. However, this excellent agreement may be fortuitous, as several authors have shown that many effects beyond the standard theory could be relevant: these include anharmonic [24] and non-adiabatic effects [32,33,45] on lattice vibrations, as well as electronic van Hove singularity

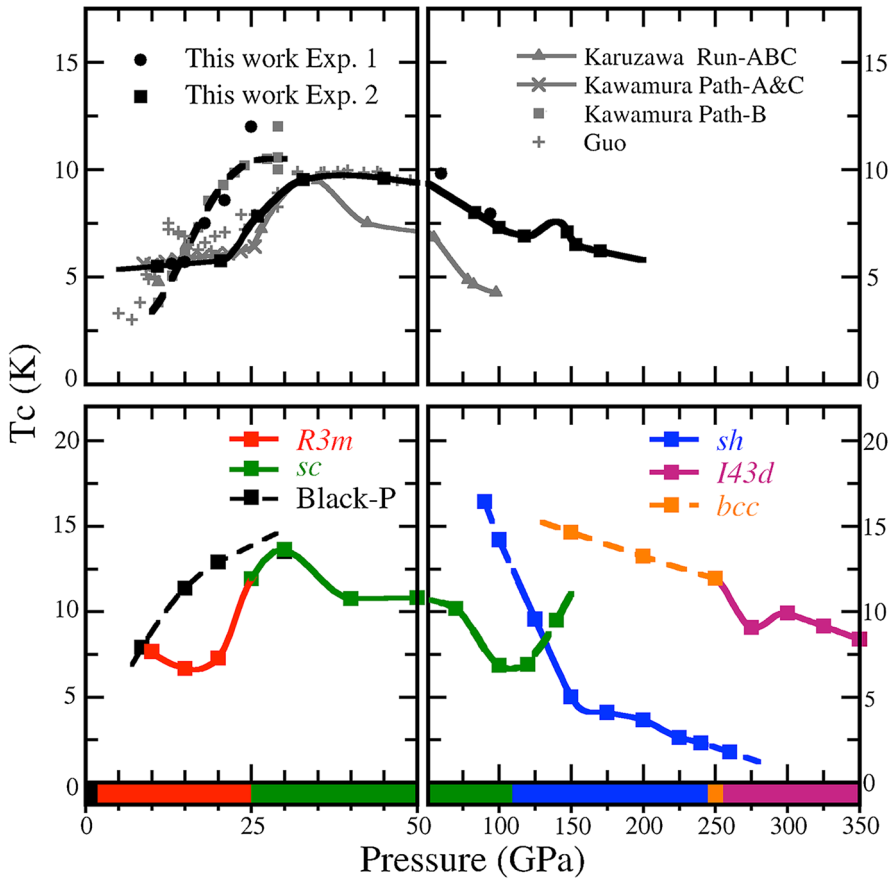

Fig. 3 High-pressure phase diagram of elemental phosphorus from resistivity measurements (*top*) and SCDFT+ minima hopping calculations (*bottom*)

effects [46]. Understanding these effects is essential, not only to improve the quantitative accuracy of description, but also because they may be exploited as alternative routes to boost the T_c.

4 Van Hove singularities in the density of states of H_3S

The band structure of H_3S in the $Im-3m$ cubic phase mainly originates from the three 1s orbitals of H, and the 3s and the three 3p orbitals of S. The 3d orbitals of S give a marginal but not negligible contribution [44]. At 5 eV around the Fermi level, these orbitals strongly hybridize [8], and therefore, the band structure is very sensitive to the H–S bond length. Indeed, the strong electron–phonon matrix element [8,44] is due to the Fermi level sitting on the region of the band structure originated from the strong H–S covalent bond [8]. The density of states shown in Fig. 4 has two hollows at $\approx \pm 2.5$ eV around the Fermi level with the emergence of a peak at the E_F. However, a zoom of the DOS around this point (inset of Fig. 4 shows a flat region of about half an eV. The DOS shows a kind of one-dimensional behavior on a large scale, while in a tiny energy range around E_F, it can be fitted using two- (three-dimensional) Van Hove singularities [44]. This puzzling feature and its consequences have not been clarified up to now.

Let us now focus on the two Van Hove singularities close to the Fermi level giving rise to the flat feature in the DOS around E_F. Indeed, tuning the energy difference Δ between the two VHs has direct consequences on the value $N(E_F)$ of the DOS at the Fermi level. Indeed, a reduction of Δ squeezes the DOS and increases $N(E_F)$ due

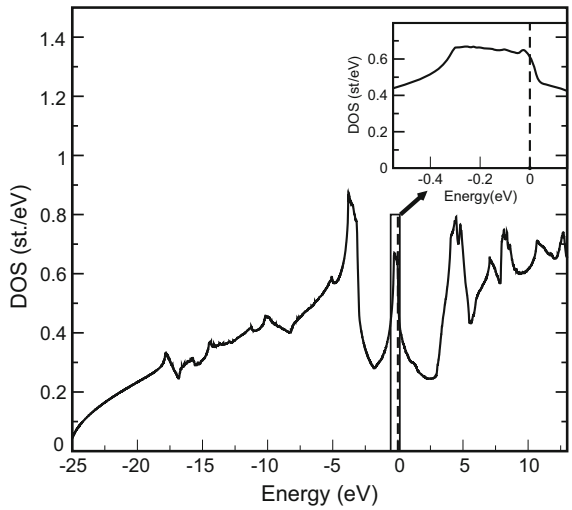

Fig. 4 Density of states (DOS) of H_3S in the $Im-3m$ cubic structure at 180 GPa. The DOS shows a kind of one-dimensional behavior on a large scale, while in a tiny energy range around the Fermi level (*inset*), it can be fitted using two- (three-dimensional) Van Hove singularities [44]

to particle number conservation (the integral of the DOS must be conserved). Vice versa, an increase of Δ causes a depression of $N(E_F)$.

The two VHs are located ≈0.01 eV above the Fermi level (first VHs) and ≈0.9 eV below E_F (second VHs), respectively. In particular, the first VHs seem to depend mainly on the S-S direct hoppings and is directly linked to the bcc coordination of the S atoms [43]. Therefore, a change in the bcc coordination of S can have drastic consequences on the DOS at the Fermi level. As noted in Refs. [1,2] indeed, the H_2S structure does not show any peak in the DOS at E_F being the S not coordinated in a bcc fashion. On the other hand, a reduction of the S 3s-S 3p direct hopping can instead lead to an increase of $N(E_F)$ due to a reduction of Δ. This is the case when S is substituted with a smaller atom like Cl [29,46].

In the next sections, we will discuss critically the role of these properties in relation to high T_c superconductivity.

5 Routes to high T_c superconductivity

Superconductivity corresponds to the onset of a state of macroscopic quantum coherence and the value of T_c defines the equilibrium point between entropy and condensation energy. At the moment, only two mechanisms for this phenomenon are known: Bose–Einstein condensation (BEC) and BCS-like theory. For the hydrides, we are clearly in the second case [8], but a brief discussion of BEC can be useful in general. Of course, we cannot exclude that other mechanisms could be identified, and for the cuprates, various hypothesis have been proposed. However, even for the cuprates, most exotic conjectures, the relation with T_c at the moment can only be done within one of these two mechanisms.

BEC describes the instability of a system of bosons and the condensation temperature is given by the following (in three dimension):

$$T_c^{\mathrm{BEC}} = \frac{2\pi\hbar^2}{k_B m}\left(\frac{n}{2.612}\right)^{2/3}, \tag{3}$$

where m is the mass of the bosons and n their density. It is remarkable that no energy or interaction potentials are involved in this expression. It is a pure configurational and statistical effect. Clearly, in superconductors, electrons are not bosons and going in this direction implies the assumption that electrons pair to form bosons above T_c and then these bosons condense at T_c. The pairing needs an interaction, but this does not appear directly in defining T_c. Such a picture implies the breakdown of the Fermi liquid well above T_c and the disappearing of the Fermi surface.

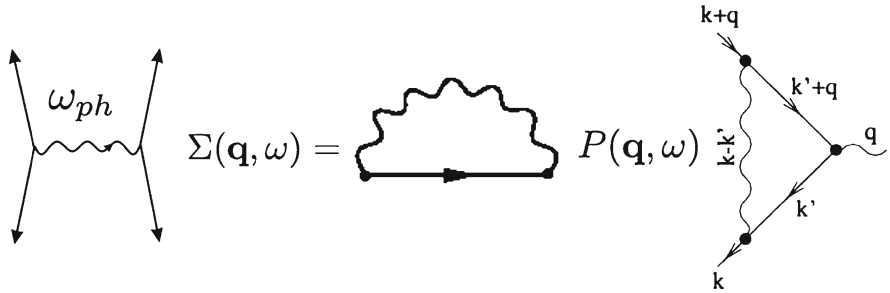

Fig. 5 Basic BCS-like diagram (*left*) self-energy diagram (*center*) and vertex correction diagram (*right*). ω_{ph} is the frequency of the phonon involved in superconductivity

Even for the most exotic cuprates, there is evidence for a Fermi surface, at least in some portion of the Brillouin zone. But, moreover, these interpretations imply that electrons are paired in real space by a very strong interaction which could be due to phonons but also to other effects. Such a situation leads unavoidably to a very large effective mass for the electron pairs which, as one can see in (3) is a handicap for the value of T_c.

Another problem is the pair density n. In the cuprates, but also in MgB_2 and in the Fullerene compounds, the electron density taking part in the onset of superconductivity is very small. This is clearly another handicap in view of Eq. (3) and, as we are going to see, also for the BCS-like mechanisms. For the hydrides, the BEC mechanisms seem to be even less likely. There is strong evidence for a well-defined Fermi surface and for a normal behavior above T_c and the coherence length is rather large [8]. So why are we mentioning BEC? Actually, precisely at this conference, Bozovic [10] has presented an exhaustive set of new data for many cuprates which show elements in the direction of the condensation of preformed pairs. This is a very interesting news which, however, cannot be interpreted directly in terms of Eq. (3). Rather, the idea would be that in some parts of the Fermi surface, there are preformed pairs and one should consider a sort of intermediate situation between BEC and BCS. In particular, he provides evidence that T_c depends more on the density rather than on the interacting energy which seems rather compelling.

Turning now to the hydrides, we are clearly in the BCS-like domain. It may be interesting then to start precisely with the standard BCS equation for T_c:

$$T_c = \omega_0 \exp(-1/\lambda)\,. \tag{4}$$

As one can easily see, inserting reasonable values for the parameters (i.e., $\omega \approx 500$–$1000\,\mathrm{K}$ and $\lambda \approx 1$) it would be very easy to get $T_c \geq 200$ K. However, nobody would discuss high T_c with this formula but rather with the McMillan equation (1) mentioned at the beginning or even a more sophisticated approach. This means that in discussing, realistically, T_c *details matter* and many body effects play a fundamental role.

Let us see how we can easily go in a simple way from BCS to McMillan. In BCS, we assume that phonons (or other possible mediators) have the only role of pairing electrons according to the standard diagram reported in Fig. 5.

However, this is not consistent, because phonons also lead to other effects like the self-energy which renormalizes the electron dispersion and introduces a finite lifetime. We can actually absorb the self-energy effect into the BCS diagram in a simple and intuitive way without resorting to the rigorous Migdal–Eliashberg (M–E) full treatment. Considering the self-energy effect, the coherent part of the electrons Green's function (the one that participates to the superconductivity in the BCS-like diagram) can be written as follows:

$$G(\mathbf{k},\omega) = \frac{1}{Z}\frac{1}{\omega - \epsilon\mathbf{k}/Z}, \tag{5}$$

where Z is the electron–phonon renormalization factor $Z = 1 + \lambda$. We can see that the self-energy effect reduces the probability that the electron propagates and also renormalizes the electron dispersion and the Fermi velocity. We can now interpret these effects in terms of effective parameters in the BCS equation (10). The vertex strength is reduced by $1/Z$ of the incoming electron, and the Fermi velocity and electron mass are changed in view of the new dispersion:

$$g^* = g/1 + \lambda \tag{6}$$
$$v_F^* = v_F/(1 + \lambda) \tag{7}$$
$$m^* = m(1 + \lambda). \tag{8}$$

In view of the smaller Fermi velocity, the density of states is increased as $N(E_\mathrm{F})^* = N(E_\mathrm{F})(1 + \lambda)$. We can, therefore, define a renormalized coupling as:

$$\lambda^* = (g^*)^2 N^*(E_\mathrm{F}) = g^2 \frac{N(E_\mathrm{F})}{1 + \lambda} = \frac{\lambda}{1 + \lambda} \tag{9}$$

and plugging Eq. (9) into the BCS expression for T_c (10), we get

$$T_\mathrm{c} = \omega_0 \exp\left(-\frac{1 + \lambda}{\lambda}\right) \tag{10}$$

which accounts for the main difference between BCS and McMillan (apart from μ^*, the residual mutual interaction) and clarifies in an instructive way why the consistent inclusion of self-energy effects leads to a drastic reduction of T_c and brings the discussion into a framework of realistic values.

These many-body effects, however, are not limited to the cases which we have considered. There is a third case (Fig. 5c) in which the extra phonon is not added to a free electron propagator line, but it happens to be in the portion of the propagator which interacts with the intermediate phonon responsible for the superconducting pairing. This effect is of the same order as the self-energy ($\propto \lambda$) and, since we have seen that the self-energy has a very important effect on the value of T_c, it is reasonable to consider also the effect of this term which is named vertex correction. In the full many body treatment of Migdal–Eliashberg, these effects are totally neglected, not because of higher order, but in view of the so-called Migdal's theorem. In fact, a simple estimate of this diagram shows that it is, indeed, linear in λ as the self-energy, but with the additional factor ω_{ph}/E_F, where ω_{ph} is the characteristic phonon frequency and E_F is the Fermi energy. Therefore, we have:

$$\Sigma(\mathbf{q}, \omega) \propto \lambda \tag{11}$$
$$P(\mathbf{q}, \omega) \propto \lambda \frac{\omega_{ph}}{E_F} = \alpha\lambda. \tag{12}$$

In normal metals, $\alpha = \omega_{ph}/E_\mathrm{F}$, which is about 10^{-2} or less and it is for this reason that these terms can be neglected (adiabatic approximation) and the M–E theory is quantitatively accurate. However, for many of the anomalous superconductors, the question of the validity of the adiabatic approximation (Born–Oppenheimer) is far from trivial. For example, in the hydrides, one of the key elements is precisely a high phonon frequency ω_{ph}. Concerning the effective appropriate value of E_F, this is not so easy to estimate for a complex band structure like that of H_3S. If the relevant band is the one that leads to a peak in the density of states, then the effective E_F would be the width of the DOS peak. In this perspective, there is a strong evidence that the adiabatic parameter $\alpha = \omega_{ph}/E_\mathrm{F}$ could be appreciably larger than zero. It is, therefore, interesting to consider the possible consequences on T_c of the non-adiabatic effects like the vertex corrections. This gives a modification of the effective vertex of type:

$$\tilde{g} = g\left(1 + \lambda \frac{\omega_{ph}}{E_\mathrm{F}} P(\mathbf{q}, \omega)\right), \tag{13}$$

where $P(\mathbf{q}, \omega)$ is a complex function which depends on the exchanged momentum and frequency, which we consider in detail later. The change in the effective vertex is linear in λ as for the self-energy. Therefore, the vertex is not a higher order effect and, since the self-energy has such a drastic effect on the value of T_c, we may conceive that a similar effect could be played by the vertex. The crucial point is whether this will be positive or negative for T_c. The effect of the self-energy is clearly always negative. The role of the vertex depends on the structure of $P(\mathbf{q}, \omega)$ whose sign is not obvious as we discuss later. Combining self-energy and vertex effects, we can generalize the expression for T_c as follows:

$$T_c \approx \exp\left(-\frac{1+\lambda}{\lambda(1+\lambda\frac{\omega_{ph}}{E_F}P(\mathbf{q},\omega))^2}\right). \tag{14}$$

This shows clearly that if $P(\mathbf{q}, \omega)$ would be positive it could lead to a remarkable enhancement of T_c with respect to the standard M–E theory.

6 Uemura diagram

A very interesting empirical diagram was introduced by Uemura [51] in relation to the cuprate superconductors and then generalized also for other systems (Fig. 6). This figure reports the superconducting T_c as a function of the magnetic penetration depth expressed as an effective Fermi temperature T_F. This gives an estimate of the number of carriers effectively participating to the superconducting state. On the right side of the diagram, we have the standard superconductors for which $\omega_{ph}/E_F \approx 0$. One can see, however, that for most of the other materials, also several considered normal, the effective T_F is very small and the adiabatic parameter cannot be considered as negligible. In particular, this is true for the cuprates, for MgB_2 and for fullerene compounds. It is interesting to note that the common element among all these systems is the very small value of the superconducting carrier density. Such a situation is very negative for T_c in the perspective of BCS or Migdal–Eliashberg theories. Indeed, a low value of the superconducting carrier density is usually associated with a small density of states and with a small screening of the residual Coulomb interaction. However, it could become an asset in the non-adiabatic perspective, because a small T_F (and hence a small E_F) could switch on non-adiabatic effects. Therefore, it would be extremely interesting to locate H_3S and other hydrides in the Uemura diagram by means of suitable experiments on the magnetic penetration depth.

7 Lessons for low-pressure superconducting materials

The remarkable discovery of a record T_c for H_3S at high pressure is of great interest per se, but it can also be a guiding line for the search of novel high T_c superconducting materials at lower or even ambient pressure. Let us examine the various elements in perspective of their role in low-pressure materials.

High phonon frequency As suggested by Ashcroft [5,6], a key point is the high phonon frequency of H vibrations due to its small mass. Actually, the H frequency $\omega_H \approx 0.2\,\text{eV}$ is perfectly comparable with that of carbon in various systems $\omega_c \sim 0.2\,\text{eV}$. Hydrogen is lighter, but carbon has stronger bonds, so this point is easy to realize. Actually, carbon is a good candidate also because of its flexibility in making many different compounds.

Large coupling λ The path in this direction is unavoidably bounded to the problem of lattice instability which for H_3S is cured by the high pressure. The natural path for a large electron–phonon interaction matrix element is to bring covalent bonds at the Fermi level [4,8,9]. To increase λ, one can eventually exploit also the presence of a large DOS at the Fermi level due to a Van Hove singularity. In H_3S, the peak in the DOS at the Fermi level is most likely associated with the presence of two three-dimensional VHs sitting near E_F [43,44,46] (see also Sect. 4) and very close in energy. For example, these effects can be combined to induce a large coupling by hole-doping two-dimensional materials where it is possible to exploiting the sudden increase of $N(E_F)$ with doping due to the

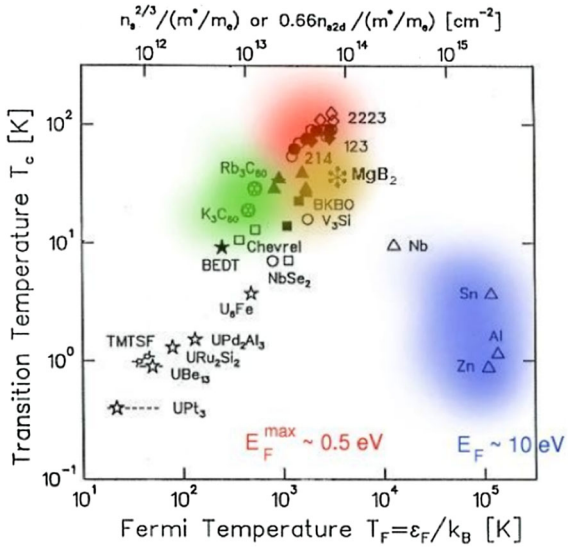

Fig. 6 Uemura diagram [51]. This diagram reports the superconducting transition temperature as a function of the effective density of electrons taking part to superconductivity measured from the magnetic penetration depth. A simple model is then used to relate this density to the Fermi energy or Fermi velocity. It is very interesting to note that the standard BCS materials are on the right and correspond to a large Fermi energy. For the fullerene compounds, we know that the charge density is very small; for A_3C_{60}, we have one electron per 20 carbon atoms. But also for the more complex cuprates, we see that the effective Fermi energy is very small. The very low carrier density is an important common element for these two classes of materials and it is an empirical hint for the possible importance of non-adiabatic effects. It would be extremely interesting to locate also H_3S on this diagram

peculiar step-like shape of the DOS with large matrix elements due to in-plane covalent bonds doped graphane [9,48].

Non-adiabatic effects Clearly, the search for optimal superconductors at low pressure acquires a new dimension if we consider also the possibility of non-adiabatic effects. A classical case are the fullerene compounds, as shown in Fig. 7. Here, we show the adiabatic parameter α as a function of the coupling λ and the reported values are from both experiments and calculations. There are many systems for which the adiabatic parameter is, indeed, negligible, and for these, the Migdal–Eliashberg theory is exact (blue line). If one moves along this line towards larger values of λ, one is expected to encounter some type of lattice instability, which, here, we indicate generically with "polaron". If we locate the A_3C_{60} compounds in this figure, using parameters obtained from experiments and realistic simulations, we find an interesting surprise. The values of λ are rather conventional ($\lambda \lesssim 1$), but the value of α is certainly different from zero and even reasonably close to 1. This is due to the high phonon frequency of the carbon modes ($\omega_{ph} \approx 0.2\,\text{eV}$) and a similar value for the Fermi energy of the half-filled LUMO bands ($E_F \approx 0.2\,\text{eV}$). In this situation, the non-adiabatic effect are certainly important and the use of the M–E theory is not justified.

These considerations for A_3C_{60} led us to study in great details the vertex function $P(\mathbf{q}, \omega)$. Before our studies, the most detailed analysis was due to Grabowsky and Sham [30] who studied only a particular limit which led to a negative value for $P(\mathbf{q}, \omega)$. This led to the conjecture that the vertex corrections would always be negative for T_c as it is the case for the self-energy. However, this is not the case.

A detailed study of the vertex function $P(\mathbf{q}, \omega)$ shown in Fig. 8, which generalizes the previous results [30], shows a very rich and interesting structure. In Fig. 8, we show the sign of the vertex function as a function of $\mathbf{q}$ and ω. This agrees with the limiting case studied in Ref. [30], but also it shows a large portion of the $(\mathbf{q}, \omega)$ space in which P is actually positive. In general, the details of $P(\mathbf{q}, \omega)$ depend on various properties like band structure, scattering matrix elements, etc. However, even the single case for which a detailed calculation is possible shows some general qualitative trends like that, for small $\|\mathbf{q}\|$, scattering P is in general positive (green region in Fig. 8).

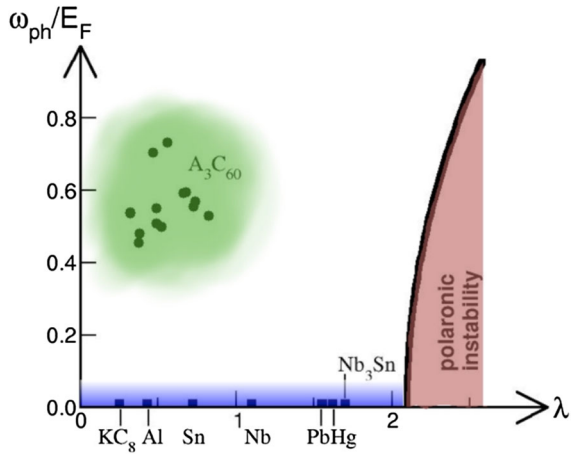

Fig. 7 Non-adiabatic phase diagram. In the *horizontal axis*, we report the coupling λ, while in the *vertical axis*, we have the adiabatic parameter. BCS theory corresponds to a situation in which the adiabatic parameter is zero and λ is small. Also in the more general Migdal–Eliashberg theory, the adiabatic parameter is zero, but λ can be relatively large. We can see from experiments and realistic calculations that for the fullerene compounds, λ is not particularly large, but the adiabatic parameter is definitely different from zero. In this situation, there is a breakdown of the standard Fermi liquid theory. Electrons still propagate as quasi particles, but they have quantum interference interactions with phonons and the Born–Oppenheimer approximation breaks down

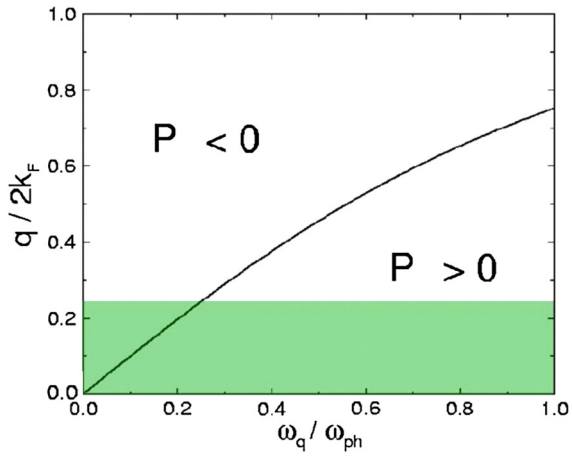

Fig. 8 Sign of the vertex function. We can see that the vertex function can be both positive and negative. If positive, it can enhance the value of T_c for superconductivity. In particular, we observe that small $\|\mathbf{q}\|$ scattering leads to positive effect. Band structure and Van Hove singularities have also important effects that have been studied in detail [32]

This result opens a new dimension in the search for optimal superconductors which is more general than the standard ME analysis. The fingerprints of non-adiabatic effects are:

- position of the material in the Uemura diagram;
- evidence of anomalous isotope effects for T_c;
- presence of an isotope effect for properties that, within the ME theory, do not possess one like for example the electron effective mass m^* and magnetic susceptibility.

We strongly suggest that experiments should be performed to check these points even in H_3S.

The possible importance of non-adiabatic effects for carbon systems at low pressure has the following consequences:

- From the above discussion of the A_3C_{60} compounds, it would be very important to try to go into acceptor compounds in which the Fermi surface is in the HOMO band. If the non-adiabatic effects are important, this could raise T_c appreciably.

– A second example is the proposal of doped graphane [48]. The idea is that a small doping in a 2-D band can lead to a high density of states. Such a situation would unavoidably place the material in the non-adiabatic framework, because E_F would be very small.

In summary, we believe that it would be important to explore the possibility of non-adiabatic effects in the hydrides at high pressure like H_3S, but, moreover, for the possible extension of these ideas to real materials at low pressure. This would give a broader scientific structure to the field but also add new original criterion for material optimization.

References

1. Akashi, R., Kawamura, M., Tsuneyuki, S., Nomura, Y., Arita, R.: First-principles study of the pressure and crystal-structure dependences of the superconducting transition temperature in compressed sulfur hydrides. Phys. Rev. B. (2015). doi:10.1103/physrevb.91.224513
2. Akashi, R., Sano, W., Arita, R., Tsuneyuki, S.: Emergent magnéli-type crystal phases and their mixture in pressurized sulfur hydride. Novel Supercond. Mater. (2017). doi:10.1515/nsm-2017-0004
3. Allen, P.B., Mitrović, B.: Theory of superconducting tc. Solid State Phys. **37**, 1–92 (1983)
4. An, J.M., Pickett, W.E.: Superconductivity ofmgb2: covalent bonds driven metallic. Phys. Rev. Lett. **86**(19), 4366–4369 (2001). doi:10.1103/physrevlett.86.4366
5. Ashcroft, N.W.: Metallic hydrogen: a high-temperature superconductor? Phys. Rev. Lett. **21**(26), 1748–1749 (1968). doi:10.1103/physrevlett.21.1748
6. Ashcroft, N.W.: Hydrogen dominant metallic alloys: high temperature superconductors? Phys. Rev. Lett. (2004). doi:10.1103/physrevlett.92.187002
7. Bednorz, J.G., Müller, K.A.: Possible hightc superconductivity in the ba–la–cu–o system. Z. Phys. B Condens. Matter **64**(2), 189–193 (1986)
8. Bernstein, N., Hellberg, C.S., Johannes, M.D., Mazin, I.I., Mehl, M.J.: What superconducts in sulfur hydrides under pressure and why. Phys. Rev. B **91**, 060511 (2015). doi:10.1103/PhysRevB.91.060511
9. Boeri, L., Kortus, J., Andersen, O.K.: Three-dimensionalmgb2-type superconductivity in hole-doped diamond. Phys. Rev. Lett. (2004). doi:10.1103/physrevlett.93.237002
10. Bozovic, I., Brown, J.A.: Following v.l. ginzburg: On the road to room temperature superconductivity. In: 2nd Annual International Workshop, Towards Room Temperature Superconductivity: SUPERHYDRIDES and MORE (2017)
11. Bustarret, E., Marcenat, C., Achatz, P., Kacmarcik, J., Lévy, F., Huxley, A., Ortéga, L., Bourgeois, E., Blase, X., Débarre, D., et al.: Superconductivity in doped cubic silicon. Nature **444**(7118), 465 (2006)
12. Carbotte, J.: Properties of boson-exchange superconductors. Rev. Mod. Phys. **62**(4), 1027 (1990)
13. Cohen, M.L., Anderson, P.: Comments on the maximum superconducting transition temperature. In: AIP Conference Proceedings, vol. 4, pp. 17–27 (1972)
14. Dalladay-Simpson, P., Howie, R.T., Gregoryanz, E.: Evidence for a new phase of dense hydrogen above 325 gigapascals. Nature **529**(7584), 63–67 (2016)
15. Dias, R.P., Silvera, I.F.: Observation of the wigner-huntington transition to metallic hydrogen. Science **355**(6326), 715–718 (2017)
16. Drozdov, A., Eremets, M., Troyan, I.: Superconductivity above 100 k in ph3 at high pressures. arXiv preprint arXiv:1508.06224 (2015)
17. Drozdov, A.P., Eremets, M.I., Troyan, I.A., Ksenofontov, V., Shylin, S.I.: Conventional superconductivity at 203 kelvin at high pressures in the sulfur hydride system. Nature **525**(7567), 7376 (2015). doi:10.1038/nature14964
18. Duan, D., Liu, Y., Ma, Y., Shao, Z., Liu, B., Cui, T.: Structure and superconductivity of hydrides at high pressures. Natl. Sci. Rev. **4**(1), 121–135 (2016)
19. Duan, D., Liu, Y., Tian, F., Li, D., Huang, X., Zhao, Z., Yu, H., Liu, B., Tian, W., Cui, T.: Pressure-induced metallization of dense (h2s)2h2 with high-tc superconductivity. Sci. Rep. **4**, 6968 (2014). doi:10.1038/srep06968
20. Durajski, A., Szczniak, R., Pietronero, L.: High-temperature study of superconducting hydrogen and deuterium sulfide. Ann. Phys. **528**(5), 358364 (2015). doi:10.1002/andp.201500316
21. Ekimov, E.A., Sidorov, V.A., Bauer, E.D., Melnik, N.N., Curro, N.J., Thompson, J.D., Stishov, S.M.: Superconductivity in diamond. Nature **428**(6982), 542–545 (2004). doi:10.1038/nature02449
22. Eremets, M., Trojan, I., Medvedev, S., Tse, J., Yao, Y.: Superconductivity in hydrogen dominant materials: silane. Science **319**(5869), 1506–1509 (2008)
23. Eremets, M., Troyan, I., Drozdov, A.: Low temperature phase diagram of hydrogen at pressures up to 380 gpa. a possible metallic phase at 360 gpa and 200 k. arXiv preprint arXiv:1601.04479 (2016)
24. Errea, I., Calandra, M., Pickard, C.J., Nelson, J., Needs, R.J., Li, Y., Liu, H., Zhang, Y., Ma, Y., Mauri, F.: High-pressure hydrogen sulfide from first principles: a strongly anharmonic phonon-mediated superconductor. Phys. Revi. Lett. (2015). doi:10.1103/physrevlett.114.157004

25. Flores-Livas, J.A., Amsler, M., Heil, C., Sanna, A., Boeri, L., Profeta, G., Wolverton, C., Goedecker, S., Gross, E.: Superconductivity in metastable phases of phosphorus-hydride compounds under high pressure. Phys. Rev. B **93**(2), 020508 (2016)
26. Flores-Livas, J.A., Sanna, A., Drozdov, A.P., Boeri, L., Profeta, G., Eremets, M., Goedecker, S.: Interplay between structure and superconductivity: metastable phases of phosphorus under pressure. Phys. Rev. Mater. **1**, 024802 (2017). doi:10.1103/PhysRevMaterials.1.024802
27. Flores-Livas, J.A., Sanna, A., Grauinyt, M., Davydov, A., Goedecker, S., Marques, M.A.L.: Emergence of superconductivity in doped h2o ice at high pressure. Sci. Rep. (2017). doi:10.1038/s41598-017-07145-4
28. Fu, Y., Du, X., Zhang, L., Peng, F., Zhang, M., Pickard, C.J., Needs, R.J., Singh, D.J., Zheng, W., Ma, Y.: High-pressure phase stability and superconductivity of pnictogen hydrides and chemical trends for compressed hydrides. Chem. Mater. **28**(6), 1746–1755 (2016)
29. Ge, Y., Zhang, F., Yao, Y.: First-principles demonstration of superconductivity at 280 k in hydrogen sulfide with low phosphorus substitution. Phys. Rev. B (2016). doi:10.1103/physrevb.93.224513
30. Grabowski, M., Sham, L.J.: Superconductivity from nonphonon interactions. Phys. Rev. B **29**(11), 6132–6142 (1984). doi:10.1103/physrevb.29.6132
31. Grimaldi, C., Cappelluti, E., Pietronero, L.: Isotope effect on m* in high-tc materials due to the breakdown of Migdal's theorem. EPL (Europhys. Lett.) **42**(6), 667 (1998)
32. Grimaldi, C., Pietronero, L., Strässler, S.: Nonadiabatic superconductivity: electron–phonon interaction beyond Migdal's theorem. Phys. Rev. Lett. **75**(6), 1158 (1995)
33. Grimaldi, C., Pietronero, L., Strässler, S.: Nonadiabatic superconductivity. ii. Generalized eliashberg equations beyond Migdal's theorem. Phys. Rev. B **52**, 10530–10546 (1995). doi:10.1103/PhysRevB.52.10530
34. Heil, C., Boeri, L.: Influence of bonding on superconductivity in high-pressure hydrides. Phys. Rev. B (2015). doi:10.1103/physrevb.92.060508
35. Kamihara, Y., Watanabe, T., Hirano, M., Hosono, H.: Iron-based layered superconductor la [o1-x f x] feas (x= 0.05- 0.12) with tc = 26 k. J. Am. Chem. Soc. **130**(11), 3296–3297 (2008)
36. Kokail, C., Boeri, L., von der Linden, W.: Prediction of high-tc conventional superconductivity in the ternary lithium borohydride system. arXiv preprint arXiv:1705.06977 (2017)
37. Kokail, C., Heil, C., Boeri, L.: Search for high-T_c conventional superconductivity at megabar pressures in the lithium–sulfur system. Phys. Rev. B **94**, 060502 (2016). doi:10.1103/PhysRevB.94.060502
38. Kolmogorov, A.N., Curtarolo, S.: Prediction of different crystal structure phases in metal borides: a lithium monoboride analog to Mgb_2. Phys. Rev. B **73**, 180501 (2006). doi:10.1103/PhysRevB.73.180501
39. Liu, H., Naumov, I.I., Hoffmann, R., Ashcroft, N., Hemley, R.J.: Potential high-tc superconducting lanthanum and yttrium hydrides at high pressure. Proc. Natl. Acad. Sci. **114**(27), 6990–6995 (2017)
40. Lüders, M., Marques, M., Lathiotakis, N., Floris, A., Profeta, G., Fast, L., Continenza, A., Massidda, S., Gross, E.: Ab initio theory of superconductivity. i. Density functional formalism and approximate functionals. Phys. Rev. B **72**(2), 024,545 (2005)
41. Lukas, H.L., Fries, S.G., Sundman, B., et al.: Computational Thermodynamics: The Calphad Method, vol. 131. Cambridge University Press, Cambridge (2007)
42. Nagamatsu, J., Nakagawa, N., Muranaka, T., Zenitani, Y., Akimitsu, J.: Superconductivity at 39k in magnesium diboride. Nature **410**(6824), 6364 (2001). doi:10.1038/35065039
43. Ortenzi, L., Cappelluti, E., Pietronero, L.: Band structure and electron-phonon coupling inh3s: a tight-binding model. Phys. Rev. B (2016). doi:10.1103/physrevb.94.064507
44. Papaconstantopoulos, D.A., Klein, B.M., Mehl, M.J., Pickett, W.E.: Cubic h3s around 200 gpa: an atomic hydrogen superconductor stabilized by sulfur. Phys. Rev. B (2015). doi:10.1103/physrevb.91.184511
45. Pietronero, L., Strässler, S., Grimaldi, C.: Nonadiabatic superconductivity. i. Vertex corrections for the electron-phonon interactions. Phys. Rev. B **52**, 10516–10529 (1995). doi:10.1103/PhysRevB.52.10516
46. Quan, Y., Pickett, W.E.: Van hove singularities and spectral smearing in high-temperature superconducting h3s. Phys. Rev. B (2016). doi:10.1103/physrevb.93.104526
47. Rosner, H., Kitaigorodsky, A., Pickett, W.E.: Prediction of high T_c superconductivity in hole-doped libc. Phys. Rev. Lett. **88**, 127,001 (2002). doi:10.1103/PhysRevLett.88.127001
48. Savini, G., Ferrari, A.C., Giustino, F.: First-principles prediction of doped graphane as a high-temperature electron-phonon superconductor. Phys. Rev. Lett. (2010). doi:10.1103/physrevlett.105.037002
49. Shamp, A., Terpstra, T., Bi, T., Falls, Z., Avery, P., Zurek, E.: Decomposition products of phosphine under pressure: Ph2 stable and superconducting? J. Am. Chem. Soc. **138**(6), 1884–1892 (2016)
50. Struzhkin, V.V.: Superconductivity in compressed hydrogen-rich materials: pressing on hydrogen. Phys. C **514**, 77–85 (2015)
51. Uemura, Y., Le, L., Luke, G., Sternlieb, B., Wu, W., Brewer, J., Riseman, T., Seaman, C., Maple, M., Ishikawa, M., et al.: Basic similarities among cuprate, bismuthate, organic, chevrel-phase, and heavy-fermion superconductors shown by penetration-depth measurements. Phys. Rev. Lett. **66**(20), 2665 (1991)
52. Wang, H., John, S.T., Tanaka, K., Iitaka, T., Ma, Y.: Superconductive sodalite-like clathrate calcium hydride at high pressures. Proc. Natl. Acad. Sci. **109**(17), 6463–6466 (2012)
53. Woodley, S.M., Catlow, R.: Crystal structure prediction from first principles. Nat. Mater. **7**(12), 937–946 (2008). doi:10.1038/nmat2321

54. Xie, Y., Oganov, A.R., Ma, Y.: Novel high pressure structures and superconductivity of Ca Li 2. Phys. Rev. Lett. **104**(17), 177,005 (2010)
55. Zurek, E., Hoffmann, R., Ashcroft, N., Oganov, A.R., Lyakhov, A.O.: A little bit of lithium does a lot for hydrogen. Proc. Natl. Acad. Sci. **106**(42), 17640–17643 (2009)